

PHYSICAL REVIEW B

CONDENSED MATTER AND MATERIALS PHYSICS

THIRD SERIES, VOLUME 62, NUMBER 7

15 AUGUST 2000-I

BRIEF REPORTS

Brief Reports are accounts of completed research which, while meeting the usual Physical Review B standards of scientific quality, do not warrant regular articles. A Brief Report may be no longer than four printed pages and must be accompanied by an abstract. The same publication schedule as for regular articles is followed, and page proofs are sent to authors.

Fe 2p absorption in magnetic oxides: Quantifying angular-dependent saturation effects

Susana Gota* and Martine Gautier-Soyer

Service de Physique et Chimie des Surfaces et Interfaces-DRECAM-DSM, Bâtiment 462 CEA Saclay, 91191 Gif-sur-Yvette, France

Maurizio Sacchi

Laboratoire pour l'Utilisation du Rayonnement Electromagnétique, Centre Universitaire Paris-Sud, Boîte Postale 34, 91898 Orsay, France

(Received 28 December 1999; revised manuscript received 10 March 2000)

We show that the absorption spectra of magnetic iron oxides (Fe_3O_4 , $\alpha\text{-Fe}_2\text{O}_3$) exhibit strong angular-dependent saturation effects when measured in the total electron yield mode. We analyze quantitatively the impact of saturation by independent evaluations of the probing depth (d), the absorption length (λ), and their ratio (λ/d). Our estimates are $d \approx 50 \text{ \AA}$, $\lambda(L_3) = 170 \text{ \AA}$, and $\lambda(L_2) = 525 \text{ \AA}$. The ratio $\lambda(L_2)/d \approx 9$ at the L_2 edge indicate that the extent of saturation is comparable to that observed in pure metallic Fe. In contrast, at the L_3 edge, saturation is considerably increased because of the reduced value of $\lambda(L_3)/d \approx 3.5$. As a consequence, quantitative magnetic studies based on linear and circular dichroism at the 2p edges of Fe in magnetic oxides must take into account and correct for saturation effects.

The problem of saturation effects related to indirect detection of the x-ray absorption spectrum (XAS), like total electron yield (TEY) or fluorescence yield measurements was brought up several years ago. However, recent applications of x-ray magnetic linear and circular dichroism spectroscopies (respectively, XMLD and XMCD) have pushed to a better understanding of this phenomenon. XMLD and XMCD find an increasing number of applications as techniques capable of supplying element-specific magnetic information. The consequences of saturation effects can be quite severe in dichroism studies, where weak magnetic signals are used to quantify parameters related to the ground-state magnetic properties. XMCD studies on Fe, Co, and Ni using the L -edge TEY spectra^{1,2} have shown that saturation can cause errors in excess of 100% on the extracted magnetic moment values.

Saturation occurs when the measured signal is no longer proportional to the photoabsorption cross section and intensities of prominent absorption peaks are reduced or "saturated." In the TEY detection mode, XAS is measured by collecting the electrons that escape from the surface as a result of the decay of the core hole.^{3,4} The ease of detection and the intense signals make TEY an extensively used technique. Although the elementary scattering processes in-

involved in TEY can be treated exactly, it is very difficult to account for the ensemble of events that can take place. Therefore, the way of predicting the probing depth, and the related surface sensitivity, for a given material remains to a large extent unclear.

Following the description given by Thole *et al.* in Ref. 5, the TEY intensity for an infinitely thick layer is given by

$$I(\alpha, E) = \frac{Ad}{d + \lambda(E) \sin \alpha}, \quad (1)$$

where A is the number of electrons produced per photon which run in the direction of the surface, α is the angle of incidence of the x rays defined relative to the sample surface, d is the probing depth, and $\lambda(E)$ is the absorption length.

The relevant parameter for angle-dependent saturation effects is the ratio between d and $\lambda(E) \sin \alpha$, the effective absorption length projected along the surface normal. For a given α and for $d \ll \lambda(E) \sin \alpha$, the measured yield is inverse proportional to the absorption length and thus proportional to the absorption coefficient (μ).

$$I(\alpha, E) \approx \frac{Ad}{\lambda(E) \sin \alpha} \propto \frac{1}{\lambda(E)} = \mu(E). \quad (2)$$

If d cannot be neglected with respect to $\lambda(E)\sin\alpha$, i.e., for grazing incidence of the photons and/or for strong absorption, this direct proportionality between I and μ is lost. The proportionality term will then be a function of the photon energy E and of the angle of incidence α , giving rise to angular-dependent saturation. For evaluating the extent to which TEY spectra can be considered representative of absorption, one can rewrite Eq. (1) as

$$I(\alpha, E)\sin\alpha = \frac{A}{\operatorname{cosec}\alpha + \lambda(E)/d}. \quad (3)$$

Indeed, $I(\alpha, E)$ scales as $\operatorname{cosec}(\alpha)$ to account for the different photon path length into the active thickness d when the angle of incidence is varied. Therefore, $I(\alpha, E)\sin(\alpha)$ gives a normalized intensity per absorbing atom that is α independent as long as the $\operatorname{cosec}\alpha \ll \lambda(E)/d$ condition is satisfied.

Equation (3) indicates that, for a given angle, saturation effects depend on λ/d . As both quantities change when going from pure metals to oxides, saturation effects are expected to be, for a given element and absorption resonance, different for metallic or oxide compounds.⁶ However, a clear trend for different materials (oxides vs metals) has not been identified yet.

Previous works have estimated saturation effects for metals at absorption resonances having large cross sections, like the $L_{2,3}$ edges of transition metals (TM) (Refs. 1, 2 and 7) and the $M_{4,5}$ edges of rare earths (RE).^{8–11} Resulting d values were found to be strongly material dependent and much shorter than expected. In contrast, quantitative studies concerning saturation effects in insulating materials and oxides are scarce.^{6,9}

Magnetic oxides are currently the focus of considerable interest because of their applications in spin electronics.¹² Oxide-based magnetic tunnel junctions are expected to make possible in the future the design of a new generation of read heads for magnetic recording and nonvolatile magnetic memories.^{12,13} The potential of XMLD and XMCD for studying their magnetic properties has been recently shown^{14–16} and, as a consequence, the impact of saturation effects needs to be considered also for this class of materials.

In this paper we address the problem of saturation effects at the Fe $L_{2,3}$ resonances of magnetic iron oxides through an independent evaluation of (λ/d) , λ , and d . Our study concerns both antiferromagnetic α -Fe₂O₃ and ferrimagnetic Fe₃O₄. Experimental procedures and analysis will be discussed in detail for the later, while results for α -Fe₂O₃ will only be given in the conclusions.

The samples were thin Fe₃O₄ layers epitaxially grown on α -Al₂O₃ (0001) single crystals by atomic oxygen assisted-MBE (molecular beam epitaxy). The thickness of the Fe₃O₄ layers ranged from 5 to 240 Å. Layers exhibit good quality LEED (low-energy electron diffraction) and RHEED (reflection high-energy electron diffraction) patterns corresponding to Fe₃O₄(111). The composition of the films was controlled by XPS (x-ray photoemission spectroscopy) at the Fe 2*p* core level. The absolute film thickness scale was calibrated independently by RHEED and by RBS (Rutherford backscattering spectroscopy). A detailed description of the films preparation procedure and characterization can be found in

previous papers.^{17–19} The samples were brought up to air before transferring to the measuring chamber. Comparison of XPS spectra taken on the same samples as prepared and after air exposure showed that, apart from some C contamination, no changes occurred in the film composition and stoichiometry.

The experiments presented in this paper were conducted at the Advanced Light Source storage ring in Berkeley, using beamline 6.3.2.²⁰ The beamline, based on a Hettrick-Underwood design, has no entrance slits to the monochromator and uses a varied line spacing grating. Beamline 6.3.2 was operated to give linearly polarized photons with a resolving power of $E/\Delta E \sim 2000$. The spot size at the sample position is about 150/30 μm horizontal/vertical. The angle of incidence of the beam on the sample could be varied continuously with a high precision, always keeping the photon polarization vector parallel to the sample surface. Fe $L_{2,3}$ spectra were obtained by measuring the sample drain current.

Figure 1 shows the maximum intensity corrected for the angle of incidence (α), at the L_3 and the L_2 resonances for an Fe₃O₄ layer 240 Å thick. In absence of saturation, $I(\alpha, E)\sin(\alpha)$ should be independent of α . On the contrary, we observe a strong reduction when the angle of incidence decreases. For a given α , the intensity is more severely reduced at the L_3 than at the L_2 edge. The two experimental curves are fitted with the expression of Eq. (3) using A and λ/d as free parameters. We found that the best fits correspond to $\lambda/d = 3.5 \pm 0.3$ at the L_3 edge and to $\lambda/d = 9 \pm 0.6$ at the L_2 edge, meaning that the $d \ll \lambda(E)\sin\alpha$ condition is better satisfied in the latter case. However, an order of magnitude between λ and d at the L_2 edge does not seem sufficient to guarantee the proportionality of the TEY spectrum to

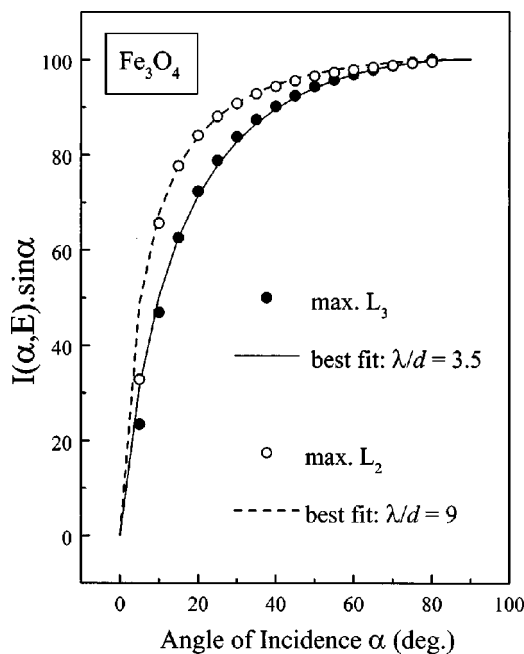


FIG. 1. $I(\alpha, E)\sin\alpha$ as a function of α for the 240 Å-thick Fe₃O₄ layer. Solid and open circles correspond respectively to the maxima of the L_3 and L_2 edges. Both intensity curves are normalized to 100 for $\alpha = 90^\circ$. Curve fittings with the expression of Eq. (3) using A and λ/d as free parameters are also shown. The best fits yield $\lambda/d = 3.5$ for the L_3 edge (solid line) and to $\lambda/d = 9$ for the L_2 edge (dashed line).

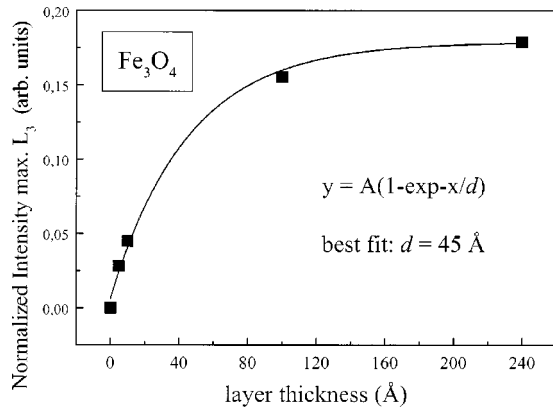


FIG. 2. Normalized peak height at the L_3 edge plotted as a function of the Fe_3O_4 layer thickness. A series of layers with thicknesses of 5, 10, 100, and 240 Å was used. The curve fitting to an exponential function giving the TEY intensity as a function of the film thickness is also plotted. The best fitting using the probing depth as a free parameter was obtained for $d = 45$ Å.

the absorption coefficient. To better evaluate the interplay of λ and d in producing saturation effects, we have tried to determine them individually.

d was experimentally estimated from the thickness-dependent values of the L_3 intensity normalized to the background before the resonance. A series of layers with thicknesses of 5, 10, 100, and 240 Å was used. Figure 2 shows the normalized peak height at the L_3 edge plotted as a function of the Fe_3O_4 layer thickness.

In the case of a thin film, the TEY intensity is given by the expression $I = (1 - e^{-x/d})I_\infty$, where x is the layer thickness and d is the TEY probing depth. I_∞ is the electron yield from an infinite thick layer, that we have approximated with the Fe_3O_4 layer 240 Å thick. The curve fitting to an exponential function $y = A(1 - e^{-x/d})$ results in a value of $d = 45 \pm 2$ Å and it is also shown in Fig. 2.

It is generally assumed that the TEY signal consists of two contributions: (i) the excited photoelectrons and Auger electrons from the decay of the core hole (elastic electrons) and (ii) the cascade of low-energy electrons produced in the inelastic scattering events. The mean probing depth is, in general, expected to combine the escape depth of both elastic and inelastic electrons. The contribution to d coming from the primary electrons is mainly related to the inelastic mean free path of the Auger electrons, notably L_{VV} , L_{MV} , and L_{MM} for the Fe $2p$ edges. For these electrons (600–700 eV) the mean free path follows well the universal curve, with values in the order of ~ 10 Å. In contrast, the d value associated to the low-energy cascade is expected to be highly material dependent: the transport of low-energy electrons, for instance, is different in a metal and in a wide gap insulator. In metals, low-energy electrons can always attain thermal equilibrium by losing energy in inelastic scattering processes involving valence-band electrons. This is the reason why d was found to be rather short in both TM and RE (10–25 Å). Recently, Nakajima *et al.* determined the TEY probing depths of 17 Å for Fe and 25 Å for Co and Ni in metallic samples.¹ In the case of TM, Siegmann proposed a model based on spin-polarized transport measurements, where the inelastic cross section is simply proportional to the

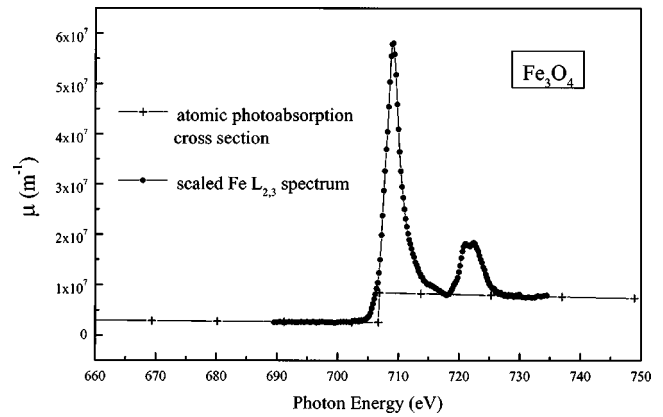


FIG. 3. Experimental Fe $L_{2,3}$ spectrum of a Fe_3O_4 layer of 240 Å of thickness (squares), scaled to the calculated atomic photoabsorption cross section of Fe_3O_4 (crosses).

number of holes in the d band.²¹ In the case of insulators, the electrons at the bottom of the conduction band have no effective mechanism for losing energy. Furthermore, in large band-gap materials, the bottom of the conduction band may be above the vacuum level, so that the electrons can readily escape from the solid.

Our estimate of $d = 45 \pm 2$ Å for Fe_3O_4 is roughly three times the value reported for pure metallic Fe ($d = 17$ Å).¹ These results give further evidence of a highly material dependent probing depth for TEY.

$\lambda(E)$ was derived by inversion of the absolute absorption intensity, obtained by scaling the experimental $L_{2,3}$ TEY spectrum measured at $\alpha = 90^\circ$ to the calculated atomic photoabsorption cross section $\mu_a^T(E)$. The latter is the weighed sum of the iron and oxygen atomic photoabsorption cross sections $\mu_a^T(E) = \mu_a^{\text{Fe}}(E) + \mu_a^{\text{O}}(E)$, to account for the atomic density of the two elements in Fe_3O_4 . Atomic values of the off-resonance cross sections were obtained from the work of Henke *et al.*²² The resulting $\mu_a^T(E)$ of magnetite is plotted in Fig. 3. It presents a step at the energy corresponding to the Fe $2p$ edge, but no fine structure related to the electronic properties. The scaled experimental TEY Fe $L_{2,3}$ spectrum shown in Fig. 3 corresponds to a Fe_3O_4 layer of 240 Å of thickness. The values obtained for $\lambda(E)$ at photon energies corresponding to the maximum of the $L_{2,3}$ edges are, respectively, $\lambda(L_3) = 170 \pm 20$ Å and $\lambda(L_2) = 525 \pm 60$ Å (error bars are mainly related to the alignment procedure). These values depend on the adopted photon energy resolution, that can affect width and height of the absorption peaks. They also rely on the hypothesis that the normal incidence spectrum is not affected by saturation: the comparison between normal incidence transmission and TEY spectra of Fe (Ref. 2) and RE (Ref. 11) shows that this condition is not fully satisfied, with saturation effects that can attain 2–5 % in TEY.

For RE and TM the cross sections can be very high, reducing $\lambda(E)$ to very low values. For the $M_{4,5}$ edges of Dy (Ref. 10) Gd, Ho, and Er (Ref. 11) experimental results agree with theoretical estimates of $\lambda(M_{4,5}) \approx 110$ –140 Å. For Fe, Co, and Ni, $\lambda(L_3) \approx 200$ Å and $\lambda(L_2) \approx 350$ Å were reported in the literature.^{23,24} In particular, the values given for pure metallic Fe are $\lambda(L_3) \approx 170$ Å and $\lambda(L_2) \approx 320$ Å.^{1,2,23} In the oxide, the reduced density of Fe tends to increase λ , whereas

that the lower $3d$ occupancy of Fe tends to decrease it. Since no systematic studies (metal vs oxides) can be found currently, it is difficult to assess the relative importance of these two factors acting in opposite directions. As a consequence, a quantitative experimental evaluation must be done for each material.

Taking into account the error bars associated to the obtained values of (λ/d) , λ , and d , we find that these independent evaluations have internal coherence. On the one hand, the ratio between λ and d values estimated individually are $\lambda(L_3)/d=170/45=3.8\pm 0.6$ and $\lambda(L_2)/d=525/45=11.7\pm 2$. These values are in good agreement with the estimations of the ratios $\lambda(L_3)/d=3.5$ and $\lambda(L_2)/d=9$ from the curve fitting of Fig. 1. On the other hand, we can derive d using $\lambda(L_3)=170\text{ \AA}$ and $\lambda(L_2)=525\text{ \AA}$ (Fig. 3) and introducing them in the ratio $\lambda(L_3)/d=3.5$ and $\lambda(L_2)/d=9$ (Fig. 1). By this procedure, we evaluate d to 48 ± 10 and $58\pm 12\text{ \AA}$, respectively.

Our study adds experimental evidence to one general aspect of TEY saturation, i.e., its material dependence. It is interesting, for instance, to look at our results for Fe_3O_4 and $\alpha\text{-Fe}_2\text{O}_3$ with reference to those reported for metallic Fe. In this latter case, the values found in the literature are $\lambda(L_3)/d=10$ and $\lambda(L_2)/d=19$.^{1,2} The reduced density of Fe

ions in iron oxides tends to increase λ , hence to weaken saturation, but the reduced $3d$ occupancy of Fe in the oxide induces stronger oscillator strengths, and acts in the opposite direction. Moreover, we have found a TEY probing depth for the oxide about three times larger than for the metal. The net result is, for a given angle, a stronger saturation for the oxide than for the metal. In the case of the L_2 edge, the increase of both $\lambda(L_2)$ and d with respect to the metal yields comparable saturation effects. At the L_3 edge, $\lambda(L_3)$ is similar in the oxide and in the metal, but d is three times larger in the former: we have found TEY probing depths of about 50 and 35 \AA for Fe_3O_4 and $\alpha\text{-Fe}_2\text{O}_3$, respectively, giving λ/d values of 3.5 and 4.5. Such small values induce strong angular-dependent saturation. As a consequence, quantitative magnetic studies based on linear and circular dichroism at the $2p$ edges of Fe in magnetic oxides must take into account and correct for saturation effects.

We want to stress, though, that our conclusions (oxide vs metal) cannot be safely generalized: as long as we have no reliable way of predicting d values, quantitative experimental studies are required for each material.

We thank C. F. Hague, J. H. Underwood, and E. M. Gullikson for their assistance during the measurements and the ALS staff for support.

*Corresponding author. e-mail: gota@drecam.cea.fr

¹R. Nakajima, J. Stöhr, and Y. U. Idzerda, Phys. Rev. B **59**, 6421 (1999).

²V. Chakarian, Y. Idzerda, and C. T. Chen, Phys. Rev. B **57**, 5312 (1998).

³A. Erbil, G. S. Cargill III, R. Frahm, and R. F. Boehme, Phys. Rev. B **37**, 2450 (1988).

⁴B. L. Henke, J. Liesegang, and S. D. Smith, Phys. Rev. B **19**, 3004 (1979).

⁵B. T. Thole, G. van der Laan, J. C. Fuggle, G. A. Sawatzky, R. C. Karnatak, and J. M. Esteva, Phys. Rev. B **32**, 5107 (1985).

⁶R. G. Jones and D. P. Woodruff, Surf. Sci. **114**, 38 (1982).

⁷J. Vogel and M. Sacchi, Phys. Rev. B **49**, 3230 (1994).

⁸J. M. Esteva, R. C. Karnatak, and J. P. Connerade, J. Electron Spectrosc. Relat. Phenom. **31**, 1 (1983).

⁹M. Abbate, J. B. Goedkoop, F. M. F. De Groot, M. Grioni, J. C. Fuggle, S. Hofmann, H. Petersen, and M. Sacchi, Surf. Interface Anal. **18**, 65 (1992).

¹⁰J. Vogel and M. Sacchi, J. Electron Spectrosc. Relat. Phenom. **67**, 181 (1994).

¹¹F. C. Vicentin, S. Turchini, F. Yubero, J. Vogel, and M. Sacchi, J. Electron Spectrosc. Relat. Phenom. **74**, 187 (1995).

¹²J. S. Moodera, L. R. Kinder, T. M. Wong, and R. Meservey, Phys. Rev. Lett. **74**, 3273 (1995).

¹³G. A. Prinz, Phys. Today **48** (4), 58 (1995).

¹⁴E. Pellegrin *et al.*, Phys. Status Solidi B **215**, 797 (1999).

¹⁵P. Kuiper, B. G. Serle, L. C. Duda, R. M. Wolf, and P. J. van der Zaag, J. Electron Spectrosc. Relat. Phenom. **86**, 107 (1997).

¹⁶P. Kuiper, B. G. Searle, P. Rudolf, L. H. Tjeng, and C. T. Chen, Phys. Rev. Lett. **70**, 1549 (1993).

¹⁷S. Gota, E. Guiot, M. Henriot, and M. Gautier-Soyer, Phys. Rev. B **60**, 14 387 (1999); S. Gota, E. Guiot, M. Henriot, and M. Gautier-Soyer, Surf. Sci. **454-456**, 796 (2000).

¹⁸E. Guiot, PhD thesis, Université P. et M. Curie, Paris VI (1998).

¹⁹E. Guiot, S. Gota, M. Gautier-Soyer, and S. Lefèbvre, in *Applications of Synchrotron Radiation Techniques to Material Science IV*, edited by S. Mini, S. R. Stock, D. L. Perry, and L. J. Terminello, MRS Symposia Proceedings No. 524 (Materials Research Society, Pittsburgh, 1998), p. 101.

²⁰J. H. Underwood, E. M. Gullikson, M. Koike, P. C. Batson, P. E. Denham, K. D. Frank, R. E. Tackaberry, and R. Steele, Rev. Sci. Instrum. **67**, 3343 (1996).

²¹H. C. Siegmann, J. Phys.: Condens. Matter **4**, 8395 (1992).

²²B. L. Henke, E. M. Gullikson, and J. C. Davis, At. Data Nucl. Data Tables **54**, 181 (1993); (see also http://www-cxro.lbl.gov/optical_constants/asf.html).

²³C. T. Chen, Y. U. Idzerda, H.-J. Lin, N. V. Smith, G. Meigs, E. Chaban, G. H. Ho, E. Pellegrin, and F. Sette, Phys. Rev. Lett. **75**, 152 (1995).

²⁴F. Yubero, S. Turchini, F. C. Vicentin, J. Vogel, and M. Sacchi, Solid State Commun. **93**, 25 (1995).